Structure and Morphology of Poly(isobenzofuran) Films Grown by Hot-Filament Chemical Vapor Deposition

Hyun-Goo Choi,[†] John P. Amara,[‡] Tyler P. Martin,[†] Karen K. Gleason,[†] Timothy M. Swager,[‡] and Klavs F. Jensen*[,†]

Department of Chemical Engineering and Department of Chemistry, Massachusetts Institute of Technology, 77 Massachusetts Avenue, Cambridge, Massachusetts 02139

Received July 13, 2006. Revised Manuscript Received October 11, 2006

We describe hot-filament chemical vapor deposition of poly(isobenzofuran) (PIBF) films and characterize their chemical structure and surface morphology. The precursor monomer, 1,2,3,4-tetrahydro-1,4-epoxynaphthalene, is pyrolyzed by flowing it over an array of hot filaments held at three different temperatures (680, 738, and 800 °C). The produced intermediate, isobenzofuran (IBF), is deposited onto a silicon substrate as thin films of PIBF. Fourier transform infrared spectroscopy and X-ray photoelectron spectroscopy revealed that the films prepared at 800 °C possess a chemical structure and a composition different from those prepared at lower filament temperatures (680 and 738 °C). Increasing filament temperature also leads to the formation of defect domains in the polymer films. By atomic force microscopy, we observe a decrease in surface roughness and in the average size of polymer grains in PIBF domains as the filament temperature is increased. Defect domains exhibit a rougher surface as well as larger size polymer grains than those in PIBF domains. Spectroscopic and microscopic results suggest that growth of the polymer in the defect domains proceeds by a mechanism different from that in the PIBF domains.

Introduction

Isobenzofuran (IBF), a highly reactive molecule, is typically generated in situ as a transient intermediate in synthetic pathways. Since the isolation and characterization of IBF by Fieser and Haddadin, there has been considerable interest in the synthetic use of this reactive intermediate.[1−4] Under ambient conditions, IBF and its derivatives can provide access to a variety of naphthalenes and heterocyclic derivatives.[3,4] Of the several methods to prepare IBF, flash vacuum thermolysis (650 °C and 0.1 Torr) of 1,2,3,4-tetrahydro-1,4-epoxynaphthalene followed by cold trapping of the generated IBF is a promising scheme due to the relatively high yield of the transformation.[5] IBF is stable at low temperature (i.e., −80 °C), but its high reactivity under ambient conditions results in polymerization.[1−5] The polymerization of IBF has been briefly mentioned in early reports of the chemistry of IBF. However, to our knowledge, IBF has never been intentionally used as a monomer for the preparation of polymeric coatings. Poly(isobenzofuran) (PIBF) and related derivatives could provide tunable optical, chemical, and electrical properties suitable for a wide range of applications. Unfortunately, the high reactivity of IBF and its derivatives leads to several undesirable byproducts and poor-quality polymers from solution-based polymerizations.

Chemical vapor deposition (CVD) processes are attractive methods for the preparation of functional polymer coatings. CVD processes present several advantages over conventional solvent-based processes, including pinhole-free, solvent-free, noncontact, and conformal coating of complex structures. Among the different CVD techniques, hot-filament CVD (HFCVD) has been used as an alternative to plasma-enhanced CVD (PECVD)[6−12] or thermal CVD[13,14] for producing silicon and organosilicon films,[15−19] fluorocarbon films,[20−23] and

* To whom correspondence should be addressed. E-mail: kfjensen@mit.edu. Fax: (617) 258-8224.
[†] Department of Chemical Engineering.
[‡] Department of Chemistry.

(1) Fieser, L. F.; Haddadin, M. J. *J. Am. Chem. Soc.* **1964**, *86*, 2081.
(2) Warrener, R. N. *J. Am. Chem. Soc.* **1971**, *93*, 2346.
(3) Haddadin, M. J. *Heterocycles* **1978**, *9*, 865.
(4) Rodrigo, R. *Tetrahedron* **1988**, *44*, 2093.
(5) Wiersum, U. E.; Mijs, W. J. *J. Chem. Soc., Chem. Commun.* **1972**, 347.
(6) Sugimoto, I. *Macromolecules* **1991**, *24*, 1480.
(7) Kim, D. S.; Lee, Y. H.; Park, N. *Appl. Phys. Lett.* **1996**, *69*, 2776.
(8) Grill, A.; Patel, V. *J. Appl. Phys.* **1999**, *85*, 3314.
(9) Leezenberg, P. B.; Reiley, T. C.; Tyndall, G. W. *J. Vac. Sci. Technol., A* **1999**, *17*, 275.
(10) Wróbel, A. M.; Walkiewicz-Pietrzykowska, A.; Hatanaka, Y.; Wickramanayaka, S.; Nakanishi, Y. *Chem. Mater.* **2001**, *13*, 1884.
(11) Lu, J.; Cheng, Z.; Zhu, X.; Zhang, L. *J. Appl. Polym. Sci.* **2002**, *84*, 729.
(12) Biloiu, C.; Biloiu, I. A.; Sakai, Y.; Suda, Y.; Ohta, A. *J. Vac. Sci. Technol., A* **2004**, *22*, 13.
(13) Kunstmann, T. H.; Angerer, H.; Knecht, J.; Vepček, S.; Mitzel, N. W.; Schmidbaur, H. *Chem. Mater.* **1996**, *7*, 1675.
(14) Vepček, S.; Kunstmann, T. H.; Volm, D.; Meyer, B. K. *J. Vac. Sci. Technol., A* **1997**, *15*, 10.
(15) Lee, M.-S.; Bent, S. F. *J. Appl. Phys.* **2000**, *87*, 4600.
(16) Pant, A.; Russell, T. W. F.; Huff, M. C.; Aparicio, R.; Birkmire, R. W. *Ind. Eng. Chem. Res.* **2001**, *40*, 1377.
(17) Lau, K. K. S.; Pryce Lewis, H. G.; Limb, S. J.; Kwan, M. C.; Gleason, K. K. *Thin Solid Films* **2001**, *395*, 288.
(18) Mahan, A. H.; Dillon, A. C.; Gedvilas, L. M.; Williamson, D. L.; Perkins, J. D. *J. Appl. Phys.* **2003**, *94*, 2360.
(19) Murthy, S. K.; Olson, B. D.; Gleason, K. K. *Langmuir* **2004**, *20*, 4774.
(20) Limb, S. J.; Labelle, C. B.; Gleason, K. K.; Edell, D. J.; Gleason, E. F. *Appl. Phys. Lett.* **1996**, *68*, 2810.
(21) Lau, K. K. S.; Gleason, K. K. *J. Fluorine Chem.* **2000**, *104*, 119.

10.1021/cm0616331 CCC: $33.50
Published on Web 12/07/2006

Scheme 1. Formation and Polymerization of IBF by the HFCVD Process

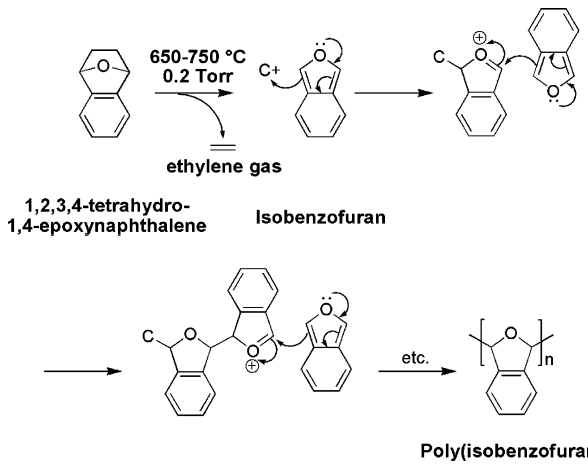

acrylate-based polymer films.[24,25] Because there are fewer reaction pathways in HFCVD than in the less selective PECVD process, HFCVD can provide better defined chemical structures of the deposited polymer films and minimizes generation of structural damage in the films.[20−22] In PECVD, UV irradiation and ion bombardment tend to create structural defects. Conventional thermal CVD involves the use of a hot pyrolysis zone, complicating the setup for polymer CVD and introducing the potential for loss of precursors to side reactions and deposition within the pyrolysis zone. Herein we demonstrate polymerization of IBF by HFCVD (see Scheme 1) and investigate structural and morphological changes of the deposited films with different filament (pyrolysis) temperatures.

Experimental Section

Materials. The precursor monomer 1,2,3,4-tetrahydro-1,4-epoxynaphthalene was either obtained from Acros Organics (Morris Plains, NJ) or synthesized according to described synthetic procedures.[26,27] Silicon wafers (4 in., p-type, 100 orientation) were purchased from Montco Silicon Technologies, Inc. (Spring City, PA). Other materials and reagents were purchased from Aldrich (Milwaukee, WI). All chemicals were of reagent grade and used as received.

Polymerization of IBF by HFCVD. Polymerization of IBF was performed by cracking 1,2,3,4-tetrahydro-1,4-epoxynaphthalene in a custom-built HFCVD system.[24,25] The precursor monomer was placed in a glass vessel and heated to 60 °C, and the vapor was flowed into the deposition chamber (10 in. in diameter and 2 in. in height) through a heated line ($T \geq 90$ °C) to prevent condensation of the precursor monomer in the transport zone. The flow rate of the vapor was regulated to 2.0 sccm by a needle valve. Pyrolysis was achieved by flowing the vapor of the precursor monomer over an array of tungsten filaments (99.95%, 0.3 mm diameter, Goodfellow, Devon, PA) that were resistively heated at constant voltages of 70, 80, and 90 V to set different pyrolysis conditions (i.e., different filament temperatures). The filament temperature was measured by a 2.2 μm infrared pyrometer[28] and confirmed by a calculation using a relationship between the resistivity and temperature of the tungsten. The reference data for the resistivity of tungsten (from the *CRC Handbook*) were plotted against temperature, and a second-order equation to fit the data was obtained (see the Supporting Information). The distance between the filament array and the substrate was 2.5 cm. PIBF films were deposited at filament temperatures of 680, 738, and 800 °C. The deposition stage holding the silicon substrate was cooled by circulating chilled water (10 °C) through internal coils on the backside of the stage. The actual surface temperature of the substrate was measured with a nine-thermocouple-bonded 4 in. silicon wafer (Thermodynamic Sensors, West Chester, PA); the reported value is an average of the measurements from nine different points on the silicon wafer at each filament temperature. For all experiments, the pressure within the deposition chamber was controlled at 0.2 Torr by a butterfly valve connected to an exhaust valve controller (type 252, MKS Instruments, Andover, MA).

Characterization of PIBF Films. The film thickness was measured by variable-angle spectroscopic ellipsometry (VASE) with a J.A. Woollam M-2000s rotating compensator ellipsometer (J.A. Woollam Co., Inc., Lincoln, NE). For each film, ellipsometric Ψ and Δ angles were measured over wavelengths from 315 to 800 nm, at three incident angles of 65°, 70°, and 75°. Subsequent regression methodology to derive the thickness and optical properties of the films were described previously.[29] The deposition was monitored in situ by interferometry using a 632.8 nm He−Ne laser. The cycle thickness was calculated by dividing the actual thickness of the polymer films by the number of cycles. Fourier transform infrared (FT-IR) spectra were obtained with a Nicolet Nexus 870 spectrometer (Thermo Nicolet Corp., Madison, WI) in normal transmission mode using a deuterated triglycine sulfate (DTGS) KBr detector over the range of 400−4000 cm^{-1} at 4 cm^{-1} resolution. X-ray photoelectron spectroscopy (XPS) spectra were obtained with a Kratos Axis Ultra spectrometer (Kratos Analytical, Chestnut Ridge, NY) equipped with a monochromatized Al Kα X-ray source. Pass energies were 160 and 10 eV for survey and high-resolution scans, respectively. All peaks were fitted with 100% Gaussian, and the peak positions were referenced to that of C(1s), 285.0 eV. Nuclear magnetic resonance (NMR) spectra were obtained on a Varian Inova 500 MHz spectrometer. All polymer solutions were filtered through 0.45 μm syringe filters prior to use, and the NMR chemical shifts were referenced to $CDCl_3$/TMS (7.27 ppm for ^1H and 77.23 ppm for ^{13}C). The molecular weight of the PIBF film was measured by gel permeation chromatography (GPC) with a Waters 1525 binary high-performance liquid chromatography (HPLC) pump (Waters, Milford, MA) equipped with an R410 differential refractometer as a detector. Polymer films were dissolved in tetrahydrofuran (THF) and filtered prior to use. Polystyrene standards from Aldrich were used for calibration, and THF was used as an eluent. Optical micrographs were obtained with an optical microscope (Nikon, TE300) equipped with a digital camera and image processing software. Surface morphologies were analyzed with a NanoScope III atomic force microscope (Digital Instruments) operating in tapping mode.

(22) Lau, K. K. S.; Caulfield, J. A.; Gleason, K. K. *Chem. Mater.* **2000**, *12*, 3032.
(23) Lau, K. K. S.; Bico, J.; Teo, K. B. K.; Chhowalla, M.; Amaratunga, G. A. J.; Milne, W. I.; McKinley, G. H.; Gleason, K. K. *Nano Lett.* **2003**, *3*, 1701.
(24) Mao, Y.; Gleason, K. K. *Langmuir* **2004**, *20*, 2484.
(25) Chan, K.; Gleason, K. K. *Langmuir* **2005**, *21*, 8930.
(26) Fieser, L. F.; Haddadin, M. J. *Can. J. Chem.* **1965**, *43*, 1599.
(27) Wittig, G.; Pohmer, L. *Chem. Ber.* **1956**, *89*, 1334.
(28) Murthy, S. K.; Gleason, K. K. *Macromolecules* **2002**, *35*, 1967.
(29) Lau, K. K. S.; Caulfield, J. A.; Gleason, K. K. *J. Vac. Sci. Technol., A* **2000**, *18*, 2404. The average value of the refractive index of PIBF films obtained by VASE is 1.63 with a standard deviation of 0.06, which is identical to that of typical PIBF films prepared by the thermal CVD process used in our previous work. This relatively high refractive index of PIBF should offer a potential application of PIBF coatings as components of optical waveguides.

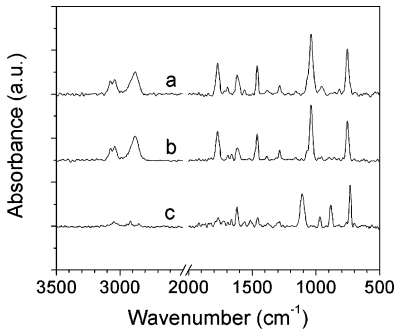

Figure 1. FT-IR spectra of PIBF films prepared at different filament (pyrolysis) temperatures: (a) $T_f = 680$ °C, (b) $T_f = 738$ °C, and (c) $T_f = 800$ °C.

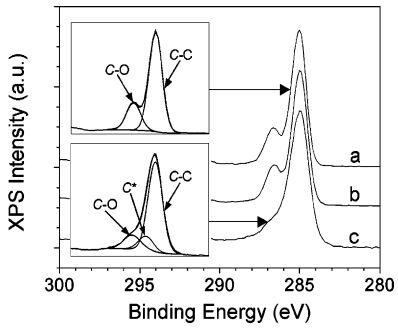

Figure 2. C(1s) high-resolution XPS spectra of the PIBF films prepared at different filament (pyrolysis) temperatures: (a) $T_f = 680$ °C, (b) $T_f = 738$ °C, and (c) $T_f = 800$ °C. The two insets represent typical examples of the curve fitting for two peak components (i.e., *C*−C and *C*−O centered at 285.0 and 286.6 eV, respectively) and three peak components (i.e., *C*−C, **C*, and *C*−O centered at 285.0, 285.6, and 286.7 eV, respectively).

Results and Discussion

FT-IR Spectroscopy. Figure 1 shows FT-IR spectra of PIBF films prepared at the different filament (pyrolysis) temperatures (T_f = 680, 738, and 800 °C). The sp^2 C−H stretch from the aromatic ring and the sp^3 C−H stretch from the polymer backbone are observed at 3040 and 2874 cm^{-1}, respectively. The C═C aromatic stretch absorptions are observed in a pair at 1615 and 1460 cm^{-1}. The furanoid C−O stretch absorptions are detected in a pair at 1285 and 1038 cm^{-1}. Other absorptions, such as weak combination/overtone bands for the *ortho*-substituted benzene (1690−1900 cm^{-1}) and an out-of-plane bending vibration for the *ortho*-substituted benzene (755 cm^{-1}), support the chemical structure of the PIBF polymer.[30,31] The PIBF films prepared at $T_f = 680$ and 738 °C show nearly identical IR spectra, whereas reductions in peak intensities and shifts in peak positions are observed from the film prepared at $T_f = 800$ °C (Figure 1c). The reduction in the peak intensities of the sp^2 C−H stretch from the aromatic ring (3040 cm^{-1}) and the sp^3 C−H stretch from the polymer backbone (2874 cm^{-1}) suggests a decrease in the degree of polymerization, which is supported by the decrease in the weight-average molecular weight of the films from 10000 ($T_f = 680$ °C) to 1000 ($T_f = 800$ °C) as determined by GPC. The shift in the peak positions of the furanoid C−O stretch (from 1038 to 1107 cm^{-1}) and the out-of-plane bending vibration for the *ortho*-substituted benzene (from 755 to 732 cm^{-1}) and the reduction of the peak intensities of the C═C aromatic stretches (a pair at 1615 and 1460 cm^{-1}) also suggest that the film possesses a chemical structure slightly different from those of the films prepared at $T_f = 680$ and 738 °C.

We observed similar results with films prepared by a thermal CVD process using a tube furnace for pyrolysis.[31] In this case, higher pyrolysis temperatures (≥800 °C) led to the generation of defects in the films that were attributed to inclusions of oligomers and decomposed materials as byproducts. To clarify the presence of different materials, we performed ^{1}H NMR analysis on the typical PIBF films and the defect-containing PIBF films. From the ^{1}H NMR spectrum of the typical PIBF films, we observed two broad peaks at 4.6−6.0 and 6.2−8.2 ppm for the protons from the furanoid ring and the aromatic protons, respectively, whereas the ^{1}H NMR spectrum of the films containing defects showed several multiplets in the 7.0−8.6 ppm range as well as two broad peaks at 4.6−6.0 and 6.2−8.2 ppm. These several multiplets in the 7.0−8.6 ppm range correspond to small molecules produced as byproducts. We speculate that these oligomeric molecules ($M_w \approx 1000$) possess structures different from that of PIBF, such as cyclic oligomers, which cannot be further polymerized.

XPS. Survey scans by XPS show that the atomic composition of this set of films is typically 86.5% (C) and 13.5% (O), which is consistent with the stoichiometry of PIBF (85.7% carbon and 14.3% oxygen). The C(1s) high-resolution scans reveal that the film prepared at $T_f = 800$ °C possesses a chemical structure different from those of the films prepared at $T_f = 738$ and 680 °C (Figure 2). The spectra of PIBF films prepared at $T_f = 680$ and 738 °C consist of two peak components corresponding to the unsaturated carbons of the aromatic ring and the oxygen-bound carbon (i.e., *C*−O in the furanoid ring), centered at binding energies of 285.0 and 286.6 eV, respectively. The area fractions of these peak components are typically 76.1% (*C*−C or *C*−H) and 23.9% (*C*−O), which are consistent with the stoichiometry of PIBF (75% *C*−C and 25% *C*−O). As the filament temperature increases to 800 °C, the area fractions of the peak components of the unsaturated carbon centered at a binding energy of 285.0 eV and the oxygen-bound carbon centered at a binding energy of 286.7 eV decrease to 74.4% and 11.8%, respectively, and a new peak component centered at a binding energy of 285.6 eV appears, with an area fraction of 13.8%. This peak at 285.6 eV is usually assigned to a carbon adjacent to either a carboxyl or an ester group when it appears along with their carbonyl peak components centered at 288.5−289.3 eV.[31,32] However, no carbonyl peak was observed from this spectrum.

We also performed ^{13}C NMR to verify whether the new peak at around 285.6 eV in high-resolution C(1s) XPS spectra is related to the presence of carbonyl in the films. We observed no sign of carbonyl carbons that usually appear

(30) Pavia, D. L.; Lampman, G. M.; Kriz, G. S. *Introduction to Spectroscopy*, 2nd ed.; Saunders College Publishing: New York, 1996; Chapter 2.
(31) Choi, H.-G.; Amara, J. P.; Swager, T. M.; Jensen, K. F. *Macromolecules* **2006**, *39*, 4400.
(32) Beamson, G.; Griggs, D. *High-Resolution XPS of Organic Polymers: The Scienta ESCA300 Database*; John Wiley & Sons: New York, 1992; pp 277−292.

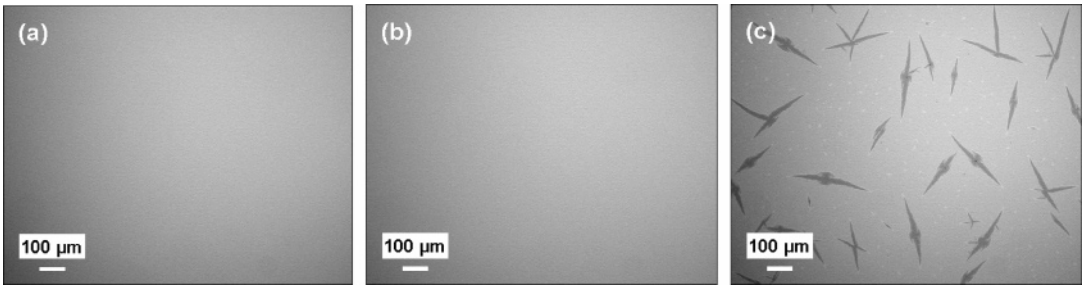

Figure 3. Optical micrographs of PIBF films prepared at different filament (pyrolysis) temperatures: $T_f = 680$ °C, (b) $T_f = 738$ °C, and (c) $T_f = 800$ °C.

between 150 and 220 ppm in ^{13}C NMR, but carbons corresponding to the benzene ring at 120−140 ppm and the furanoid ring (polymer backbone) at 86 ppm were present in the ^{13}C NMR spectrum. These results also support the generation of different materials under a higher filament (pyrolysis) temperature as observed in the IR spectrum. We previously observed similar XPS spectra for the films grown by a thermal CVD process using a tube furnace for pyrolysis, where the films were prepared at higher pyrolysis temperatures (≥800 °C) or lower vaporization temperatures for precursor material (≤50 °C). Both cases are suspected to provide excess thermal energy to the pyrolysis zone, and we ascribe the new peak centered at a binding energy of 285.7 eV to another type of C−O bond present in polymerization byproducts.[31]

The pyrolysis of the precursor monomer is a critical step to the generation of the IBF monomer, and the growth of PIBF is believed to be a self-initiated cationic polymerization process.[31] As the filament (pyrolysis) temperature increases, there should be more IBF monomer available for polymerization, and thereby, the deposition (growth) rate of the polymer should increase accordingly.[20,24,25,33] However, the deposition (growth) rate of PIBF films decreases from $k = 1.23$ Å/s ($T_f = 680$ °C) to $k = 0.54$ Å/s ($T_f = 738$ °C) and $k = 0.22$ Å/s ($T_f = 800$ °C)[34] with increased filament temperature. This result suggests that polymer growth under these operating conditions is limited by another process, such as adsorption of the IBF monomer onto the surface, rather than pyrolysis to generate the IBF monomer. Increasing the filament temperature leads not only to more IBF monomer available for polymerization but also to higher surface temperatures (T_s) as a result of increased heat transfer from the hot-filament array. This latter effect is reflected by the surface temperature measurements.[35] When the reactive IBF monomer available for the polymerization is present in sufficient quantity, the adsorption process of the IBF monomer becomes the limiting step governing the overall polymerization as the adsorption efficiency of the IBF monomer is critical to initiation (generation of propagation centers/nucleation sites for polymerization) as well as propagation of polymerization. The heat transfer from the filament array to the deposition surface makes it difficult to clearly separate the effects of filament and surface temperatures on the kinetics of film growth. Nevertheless, the deposition of PIBF films appears to be primarily dependent on the surface temperature and to follow a surface growth mechanism similar to that observed for thermal CVD of PIBF in which the deposition zone is separated from the pyrolysis zone (tube furnace).[31]

Surface Morphology. The PIBF films prepared at $T_f = 680$ and 738 °C show defect-free surfaces, whereas disordered dendritic growth of defects is observed in the film prepared at $T_f = 800$ °C (Figure 3). We suspect that the different materials generated as byproducts at a higher filament (pyrolysis) temperature are unreactive species that cannot be polymerized. The adsorption and accumulation of these unreactive species on the surface would trigger deactivation of incoming reactive species (i.e., IBF) and provide unfavorable reaction environments for polymerization of IBF. Thus, the polymer growth in the sites occupied by these unreactive species would be less effective than that in the sites occupied by the reactive species. Consequently, the sites occupied by the unreactive species would develop into defects in the films upon the further accumulation of the unreactive species.[31]

Figure 4 shows the surface morphology of PIBF films obtained under different filament temperatures. As the filament temperature increases from 680 to 738 °C, the PIBF films demonstrate smoother surfaces, as evidenced by the decrease in the average grain size from 75 to 50 nm and the average rms roughness from 4.4 to 3.2 nm. These changes in surface morphology could be caused by the increased thermal radiation from the hot-filament array with higher filament temperatures, which results in an effect similar to thermal annealing of the growing polymer chains. The decrease in the average rms roughness to 1.2 nm in the film prepared at $T_f = 800$ °C ($T_s = 85.6$ °C) could similarly be attributed to a thermal annealing effect from the hot-filament array.

Figure 5a shows a typical AFM image of defect-embedded films prepared at $T_f = 800$ °C (scan size of 100 μm × 100 μm). Unlike the film prepared by a thermal CVD process using a tube furnace with a pyrolysis temperature of 800 °C and a deposition temperature of 10 °C, of which the depth of the defects is a few hundred nanometers as evidenced by section analysis, the depth of the defect domain in the film prepared at $T_f = 800$ °C by the HFCVD process is about 20

(33) Pryce Lewis, H. G.; Caulfield, J. A.; Gleason, K. K. *Langmuir* **2001**, *17*, 7652.
(34) The thicknesses of the films prepared at $T_f = 680$, 738, and 800 °C were about 180, 170, and 110 nm, respectively.
(35) The surface temperature increases from $T_s = 56.2$ °C ($T_f = 680$ °C) to $T_s = 70.7$ °C ($T_f = 738$ °C) and $T_s = 85.9$ °C ($T_f = 800$ °C) with increased filament temperature although the stage is cooled by circulating chilled water (10 °C), indicating that the heat transfer from the hot-filament array to the surface is greater than the cooling capacity.

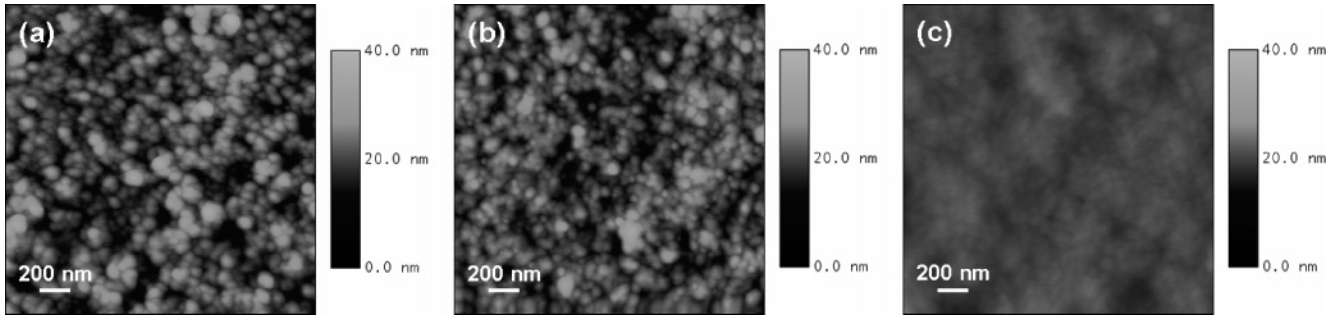

Figure 4. AFM images of the PIBF films prepared at different filament (pyrolysis) temperatures: (a) $T_f = 680$ °C, (b) $T_f = 738$ °C, and (c) $T_f = 800$ °C. All images were obtained in tapping mode with a scan size of 2 μm × 2 μm and a scan rate of 1.2 Hz.

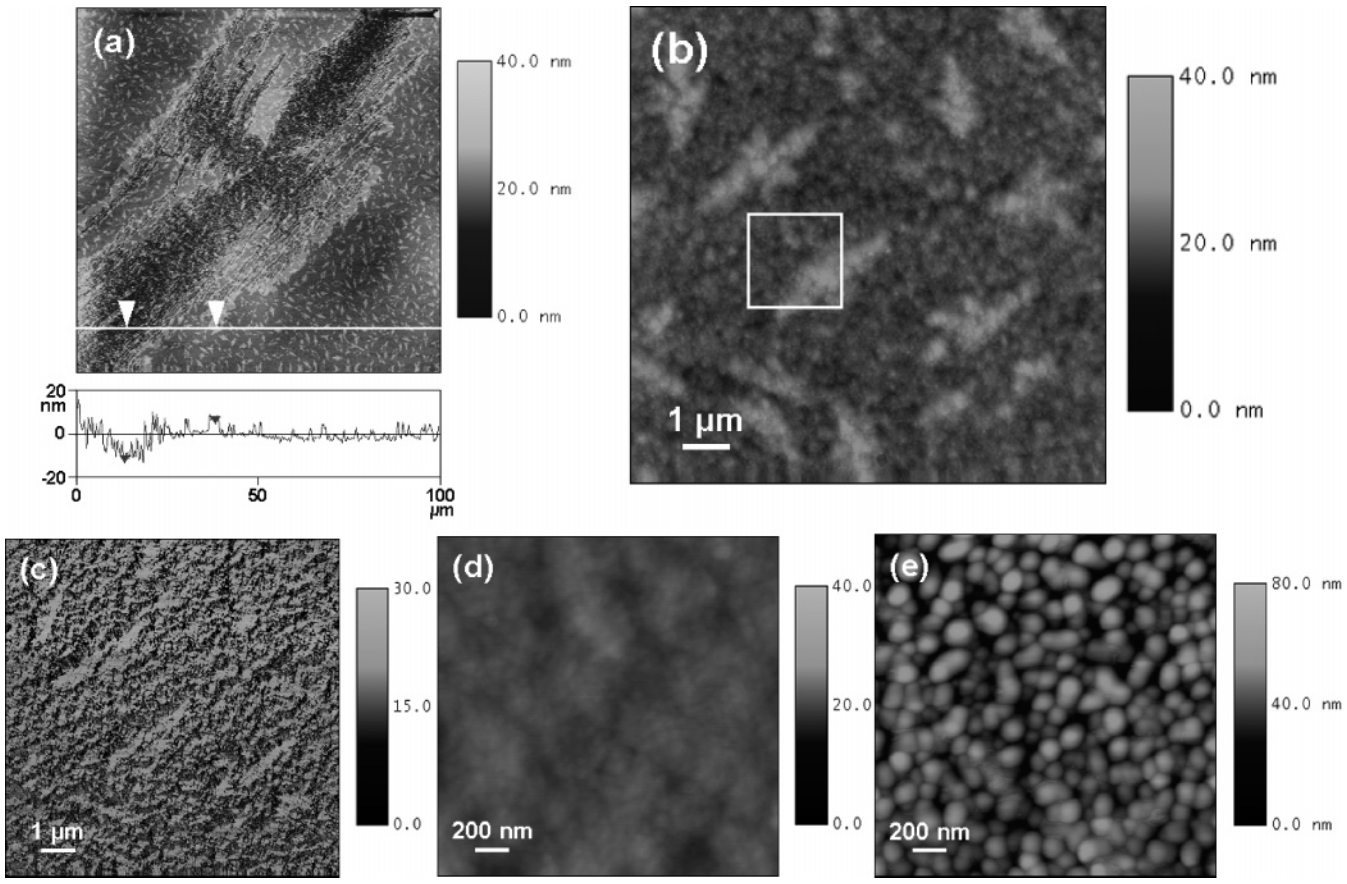

Figure 5. AFM images of a defect-embedded film prepared at $T_f = 800$ °C (a) and its surface morphologies (b−e). Micrograph c is a phase image corresponding to topographic image b. Micrograph d is a magnified scan image of the part assigned by a white square in topographic image b. Micrograph e is a topographic image of the defect domain. All images were obtained in tapping mode with a scan rate of 1.2 Hz.

nm. This behavior could be rationalized in terms of annealing by the heat radiation from the hot-filament array to the growing films. Figure 5b shows a topographic image with a scan size of 10 μm × 10 μm. It appears that small features similar to the defects are embedded in the film although the phase image (Figure 5c) corresponding to Figure 5b reveals that there is no significant difference across the scanned area. It is not clear whether these small features can develop into a large defect domain. Figure 5d is a magnified scan image of Figure 5b with a scan size of 2 μm × 2 μm, where grains with an average size of 40 nm are uniformly distributed and an rms roughness of 1.2 nm is obtained. The small grains could also result from thermal annealing during the deposition. On the other hand, much larger grains with an average size of 120 nm are observed in the defect domain with an rms roughness of 7.2 nm (Figure 5e), suggesting that the growth mechanism of the defect domain is somewhat different from that of the PIBF domain. The large grains in the defect domain suggest that there are fewer nucleation sites for growth, which results in the formation of fewer grains growing to larger sizes before coalescence.[31,36] Comparing the morphology of this defect domain with that of the film prepared by the thermal CVD process using tube furnace for pyrolysis,[31] the films prepared by the HFCVD process exhibit a more uniform distribution of grain size in defect domains than those prepared by thermal CVD, which is attributed to the effect of thermal annealing from the hot-filament array.

(36) Vaeth, K. M.; Jensen, K. F. *Chem. Mater.* **2000**, *12*, 1305.

Conclusions

The HFCVD process enables the IBF monomer to be coated as high-quality thin polymer films, but the window of operating conditions to obtain defect-free films is narrow. Such coatings cannot be realized by conventional solvent-based processes. IR and XPS analyses reveal that the chemical structure of PIBF films prepared by HFCVD is retained and nearly identical to that of films prepared by a thermal CVD process. The growth of PIBF films by HFCVD appears to follow a surface growth mechanism, where the surface temperature is a critical variable strongly affecting the growth rate and the molecular weight while the filament temperature greatly influences the surface morphology of PIBF films via thermal annealing resulting from thermal radiation from the filaments to the silicon substrate. As coatings, the polymeric thin films of IBF and its derivatives prepared by HFCVD could be useful in optical, microfluidic, and electronic devices.

Acknowledgment. This work was supported by the U.S. Army through the Institute for Soldier Nanotechnologies (ISN) under Contract DAAD-19-02-0002 with the U.S. Army Research Office and in part by the MRSEC program of the National Science Foundation under Award Number DMR 02-13282. T.M.S. acknowledges support from the Office of Naval Research MURI program.

Supporting Information Available: Additional information as noted in the text (PDF). This material is available free of charge via the Internet at http://pubs.acs.org.

CM0616331